

Growth of Si Clathrate Films with Various Annealing Conditions

K. Tanaka¹, R. Kumar², T. Maeda¹, F. Ohashi^{1,3}, H. S. Jha³, T. Kume^{1,2,3,4}

¹*Dept. of Energy Engineering, the Graduate School of Natural Science and Technology,*

²*Div. of Environmental and Renewable Energy Engineering Systems, The Graduate School of Engineering,*

³*Dept. of Electrical, Electronic and Computer Engineering, Faculty of Engineering,*

⁴*International Joint Department of Integrated Mechanical Engineering of IITG and GU, the Graduate School of Engineering, Gifu University, 1-1 Yanagido, Gifu, 501-1193 Japan.*

E-mail: kume@gifu-u.ac.jp

(Received October 4, 2019)

Si clathrate thin films were fabricated by using Si(111) substrates, Na lumps and NaH powder at various conditions in two steps annealing process. The duration of the first annealing to prepare precursor films affected the thickness and the surface morphology of the final products, i.e., Si clathrate films. The annealing duration of 18 h led to Si clathrate films of 1 - 2 μm in thickness. Attempts to control the rate of reduction of Na from the precursor films were carried out in the second step annealing under vacuum. The obtained results suggested that the rate of Na reduction affects the structure type (type I or II) of clathrate.

1. Introduction

Si clathrates [1-13] have void-rich open structures of sp^3 bonded Si, in which nanometer-size polyhedral cages are fitted. Each cage can offer the single guest atom “M”. The most familiar clathrates are type I and II [2-10]. Type I (type II) Si clathrate consists of two Si_{20} cages and six Si_{24} cages (sixteen Si_{20} cages and eight Si_{28} cages) and is formulated with M_8Si_{46} ($\text{M}_{24}\text{Si}_{136}$) if the guests fully occupy the cages [2-10]. The guest atoms are typically alkaline or alkaline earth metal [2]. In the case of type II Si clathrate with Na guests, the Na atoms partially occupy the cages, yielding $\text{Na}_x\text{Si}_{136}$ with $x = 0 \sim 24$ [4-10,12,13]. The reduction of Na can be achieved by heat treatment under vacuum. Type II Si clathrate without guests (guest free type II Si clathrate, Si_{136}) is expected to show a wide band gap nature of 1.9 eV with direct transition [12,13]. Such characteristics have increasingly attracted attention due to the potential application of Si clathrate material to visible optical devices such as lasers, solar cells and so on. However, device fabrication has been rarely reported because of the difficulty in synthesizing the clathrate in the film form.

Our research group has attempted to prepare type II Si clathrate thin films by using Si wafer as a starting material [14-17]. A method that consists of two-step annealing was proposed for the growth of clathrate films. The first step of annealing under Ar atmosphere, “Ar annealing”, was conducted for the synthesis of precursor films, and then the second step of annealing under vacuum, “vacuum annealing” was performed for the formations of clathrate structures, resulting from the thermal decompositions of the precursor films. However, the fabricated films were not suitable for practical application in a sense of quality and reproducibility. In addition, type I Si clathrate is occasionally included as the secondary phase in the prepared film. Thus, there is still room to explore the best condition for the synthesis of type II Si clathrate thin film.

In this paper, in order to gain insight into the synthesis conditions suitable for type I and II Si



clathrate films, we synthesized the film samples under various Ar-annealing and vacuum-annealing conditions. The synthesized films were characterized by X-ray diffraction measurements, Raman scattering spectroscopy, and laser microscope.

2. Experimental method

The type I ($\text{Na}_8\text{Si}_{46}$) and type II ($\text{Na}_x\text{Si}_{136}$) Si clathrates have been synthesized so far through the following steps: (1) synthesizing of Zintl phase sodium silicide (NaSi) as a precursor, (2) thermal decomposition of NaSi into type I or II Si clathrate[1]. In this paper, for synthesis of Si clathrate films, diamond structured Si(111) wafers were used as Si source. At first, as shown in Fig. 1 (a), Na lumps and NaH powder were placed at the bottom of Ta crucible and the Si wafers were placed about 10 mm above from the bottom. The Ta crucible was sealed in a stainless steel container. The above manipulations have been made under Ar atmosphere in a glove box. The setup was transferred into a muffle furnace and heated at 560°C for 12 - 48 h. This Ar-annealing process formed the precursor film of the Zintl phase NaSi. The stainless steel container was transferred again into the glove box, and the precursor films picked out from the container was then placed into a quartz tube. The tube was sealed by attaching a valve, and connected to a vacuum system with a rotary pump and a turbo molecular pump as shown in Fig. 1 (b). The quartz tube was pumped down to 10^{-3} Pa and heated using an electric furnace at 400°C for 3 h. During this vacuum-annealing process, Na is evaporated and reduced from NaSi precursor film, leading to the transformation to type I ($\text{Na}_8\text{Si}_{46}$) or type II ($\text{Na}_x\text{Si}_{136}$) Si clathrate films.

An attempt to control the reduction rate of Na from the NaSi during vacuum annealing, a receptacle made of BN with the lid was used as shown in Fig. 1 (b). Since the lid does not completely seal the receptacle, the inside of the receptacle can be evacuated in the quartz tube. The Na reduction rate for the samples inside the BN receptacle is considered to be less than those without the use of BN receptacle. After the vacuum annealing, the samples were taken out from the quartz tube and ultrasonic cleaning was conducted with deionized water for 10 min.

The obtained films were characterized by a grazing incidence X-ray diffraction (GIXRD) measurements (Rigaku, Smartlab) with $\text{Cu K}\alpha$ (9 kW) radiation and Raman scattering spectroscopy (JASCO, NRS-2100G) with 532 nm excitation. In addition, the surface morphology of the sample was investigated by a laser microscope (Keyence, VK-X200).

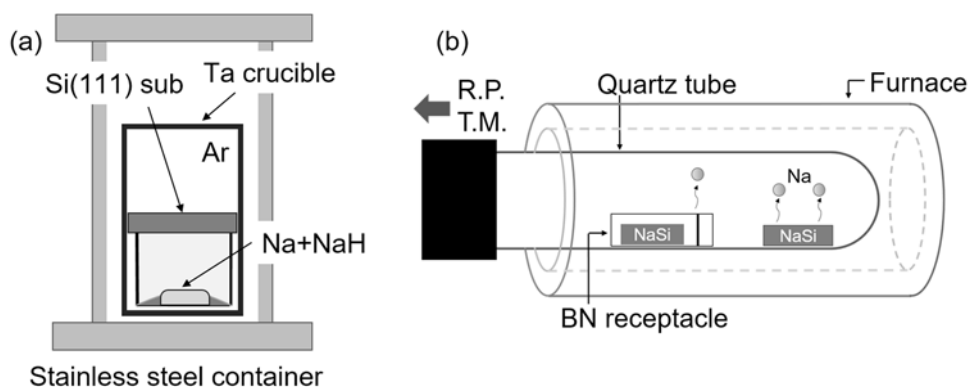


Fig. 1. The schematic setup used for (a) Ar annealing for the thermal decomposition of precursor and (b) vacuum annealing for the thermal decomposition of clathrate from precursor.

3. Result and discussion

3.1 Samples synthesized with various Ar annealing durations

Figure 2 (a) shows GIXRD patterns of Si clathrate films grown with Ar annealing durations of 12 - 48 h followed by vacuum annealing without BN receptacle. The XRD peaks from Na doped type I ($\text{Na}_8\text{Si}_{46}$) and II ($\text{Na}_x\text{Si}_{136}$) Si clathrates were observed when Ar annealing durations were 18, 24, and 48 h. The obtained films were found to be mixtures of type I and II Si clathrates. However, no peak appeared for 12 h Ar annealing. Figures 2 (b) and (c) show laser microscope images and their cross-sectional profiles of the samples for 48 h and 18 h Ar annealing, respectively. The lines A – B and C – D in the microscopic images are traces along which the cross-sectional profiles were displayed in top panels in figures (b) and (c), respectively. In Fig. 2 (b), the bright parts correspond to the surface of Si substrate exposed due to the peeling of the films during ultrasonic cleaning. The Si clathrate films correspond to the rough textured parts appearing as dark or grayish parts. Apart from the dark parts, the relatively flat surface appeared as grayish part and the thickness was estimated as 3 - 4 μm . For the sample for 18 h Ar annealing [Fig. 2 (c)], the bright parts of Si substrate appeared only in a limited area, and most parts were covered with films having small roughness compared to the above mentioned film grown with 48 h Ar annealing. The thickness of the films was estimated approximately as 1 - 2 μm . Thus, we found that the longer Ar annealing duration results in the thicker clathrate films but the thicker film has a rough surface and easily peels off the substrate.

3.2 Samples synthesized with modified vacuum annealing condition

In order to modify the vacuum annealing conditions, BN receptacle was used to keep higher Na vapor pressure in the area surrounding the sample. Figure 3 shows GIXRD patterns of the films prepared

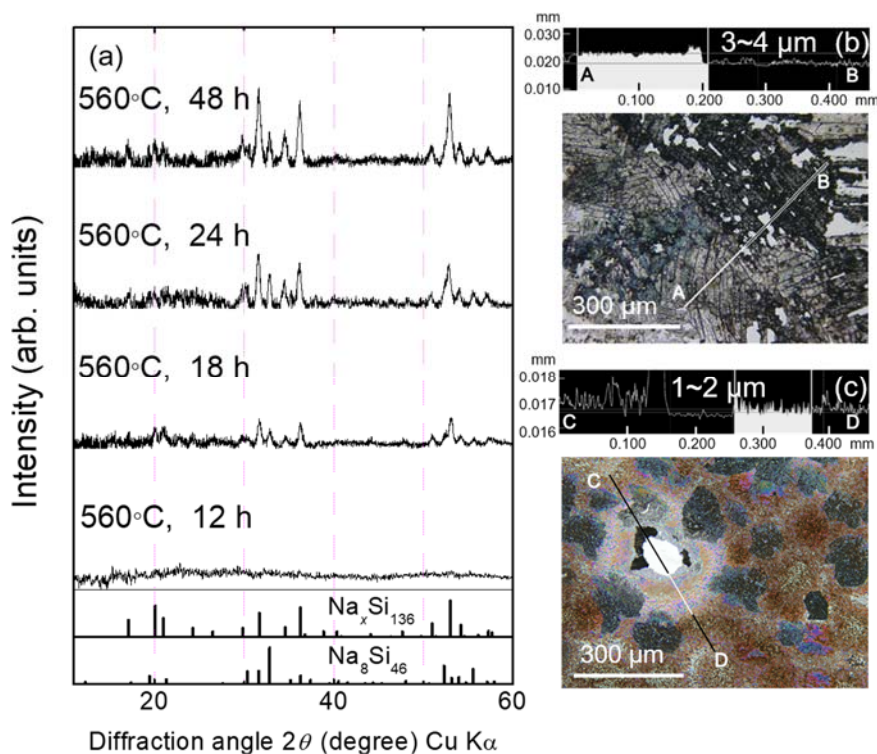


Fig. 2. (a) XRD patterns of samples with Ar annealing for 12-48 h, (b) Laser microscope image and their cross-sectional profile of clathrate films grown on Si substrate with Ar annealing for (b) 48 h and (c) 18 h.

with and without BN receptacle. The data of the samples with Ar annealing for 18, 48 h are indicated. XRD peaks originated from both types I and II Si clathrate were observed for all the samples. We find that the samples with BN receptacle show relative intensities ($I_{\text{typeI}}/I_{\text{typeII}}$) of the strongest peak of type I (at $2\theta = 32.8^\circ$) to that of type II (at $2\theta = 52.8^\circ$) always stronger than those without BN receptacle. This means that the use of BN receptacle tends to synthesize favorably type I Si clathrate.

Next, we focus on the sample with Ar annealing for 18 h and conducted Raman measurements. Figures 4 (a) and (b) show photo images of the sample prepared with and without BN receptacle, and (c) shows Raman spectra obtained from those samples. The red circles in Fig. 4 (a) and (b) depict the points where the Raman spectra were obtained. From comparison with the typical Raman spectra of type I and II Si clathrate in the bottom of figure (c), type I Si clathrate was found to be included in all the points in the sample with BN receptacle (p1-p3). (p2 corresponds to the mixture of type I and II.) On the other hand, in the case of the sample without BN receptacle (p4-p7), type II Si clathrate was only detected in p4, and type I Si clathrate was the main phase in p5 and p6. The p7 indicated only the Raman spectrum of diamond structured Si, which is possibly due to delamination of the film or no growth of Si clathrate.

The present results suggest that the use of BN receptacle leads to the growth of type I Si clathrate more preferably than type II. According to Horie *et al.* [18], there are preferable annealing conditions for the growth of type I ($\text{Na}_8\text{Si}_{46}$); type I tends to be synthesized if NaSi is annealed under high Na vapor pressure. High Na vapor pressure during vacuum annealing is considered to achieve a slow rate for Na reduction from NaSi precursor. Similar conditions were possibly realized in our experiments by using BN receptacle during vacuum annealing. Therefore, type I Si clathrate was observed in many points.

It should be noted here that the present films included type I Si clathrate even without BN receptacle, in disagreement with our previous work [16]. In the previous work, type II Si clathrates only have been generated on Si (111) substrate when the thicknesses were

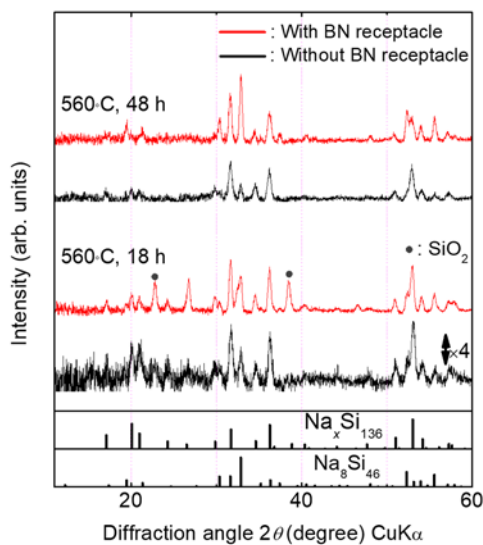


Fig. 3. XRD patterns of Si clathrate films grown with/without BN crucible during vacuum annealing.

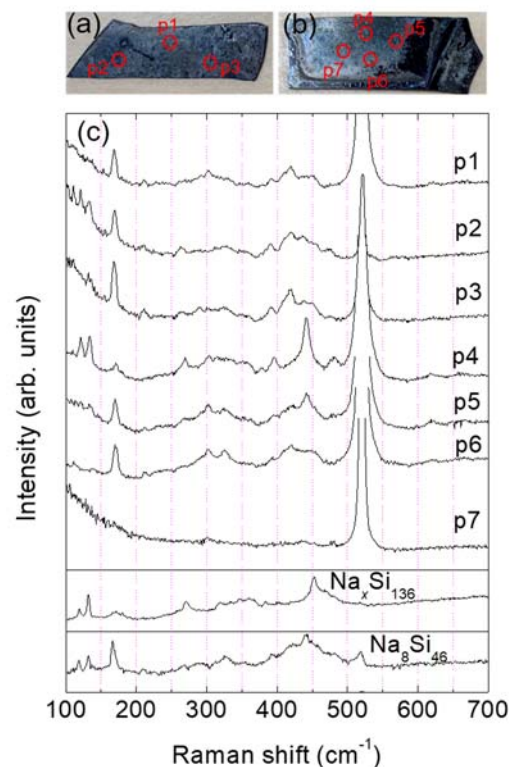


Fig. 4. Photographs of sample with Ar annealing for 18 h with (a) and without (b) BN crucible and (c) Raman spectra measured at point 1 to 7 depicted in (a) and (b).

several microns or less. This discrepancy is likely to come from the difference in Na vapor pressure during the vacuum annealing. The presence of BN receptacle in the front side of the quartz tube [Fig. 1(b)] disturbs evacuating from the bottom side, resulting in higher pressure. On the other hand, previous experiments have employed no BN receptacle. The present results and the comparison with previous work made us aware of a possibility that the structure type of Si clathrate is controlled with vacuum conditions even in the film forms.

4. Conclusion

The various conditions of Ar annealing and vacuum annealing was attempted to understand the growth mechanism of Si clathrate films. The change in the Ar annealing durations resulted in the variations in the film thickness. Thicker films gave rise to the easy delamination and rough surface. The Ar annealing duration of 18 h led to the relatively uniform film of Si clathrate. The attempt to control the rate of Na reduction in vacuum annealing were performed by using BN receptacles. The use of the receptacle led to the growth of type I Si clathrate more preferably than type II, suggesting the control of Na reduction rate from the NaSi precursor.

Acknowledgment

This work was financially supported by the Advanced Low Carbon Technology Research Project and Development Program (ALCA) of the Japan Science and Technology (JST) and Grants-in-Aid for Scientific Research (JP16K21072 and JP17H03234) of Japan Society of the Promotion of Science (JSPS).

References

- [1] J. S. Kasper, P. Hagenmuller, M. Pouchard, and C. Cros, *Science*. **150** (1965) 1713.
- [2] S. Bobev and S. C. Sevov, *J. Solid State Chem.* **153** (2000) 92.
- [3] K. A. Kovnir and A. V. Shevelkov, *Russ. Chem. Rev.* **73** (2004) 923.
- [4] G.S. Nolas, C.A. Kendziora, J. Gryko, J. Dong, C.W. Myles, A. Poddar, and O.F. Sankey, *J. Appl. Phys.* **92** (2002) 7225.
- [5] G.S. Nolas, M. Beekman, J. Gryko, G.A. Lamberton Jr., T.M. Tritt, and P.F. McMillan, *Appl. Phys. Lett.* **82** (2003) 910.
- [6] A. Ammar, C. Cros, M. Pouchard, N. Jaussaud, J.-M. Bassat, G. Villeneuve, M. Duttine, M. Ménétrier, and E. Reny, *Solid State Sci.* **6** (2004) 393.
- [7] L. Krishna, L.L. Baranowski, A.D. Martinez, C.A. Koh, P.C. Taylor, A.C. Tamboli, and E.S. Toberer, *CrystEngComm* **16** (2014) 3940.
- [8] K.A. Kovnir and A.V. Shevelkov, *Russ. Chem. Rev.* **73** (2004) 923.
- [9] M. Beekman and G. S. Nolas, *J. Mater. Chem.* **188** (2008) 42.
- [10] G. K. Ramachandran, J. Dong, J. Diefenbacher, J. Gryko, R. F. Marzke, O. F. Sankey, and P. F. McMillan, *J. Solid State Chem.* **145** (1999) 716.
- [11] K. Moriguchi, S. Munetoh, and A. Shintani, *Phys. Rev. B.* **62** (2000) 7138.
- [12] K. Moriguchi, S. Munetoh, and A. Shintani, *Phys. Rev. B.* **64** (2001) 195409.
- [13] J. Gryko, P.F. McMillan, R.F. Marzke, G.K. Ramachandran, D. Patton, S.K. Deb, and O.F. Sankey, *Phys. Rev. B.* **62** (2000) R7707.
- [14] F. Ohashi, Y. Iwai, T. Sugiyama, M. Hattori, T. Ogura, R. Himeno, T. Kume, T. Ban, and S. Nonomura, *J. Phys. Chem. Solids.* **75** (2014) 518.
- [15] T. Kume, Y. Iwai, T. Sugiyama, F. Ohashi, T. Ban, S. Sasaki, and S. Nonomura, *Phys. Status Solid C.* **10** (2013) 1739.
- [16] T. Kume, F. Ohashi, K. Sakai, A. Fukuyama, M. Imai, H. Udonon, T. Ban, H. Habuchi, H. Suzuki, T. Ikari, S. Sasaki, and S. Nonomura, *Thin Solid Films* **609** (2016) 30.
- [17] T. Kume, F. Ohashi, and S. Nonomura, *Jpn. J. Appl. Phys.* **56** (2017) 05DA05.
- [18] H. Horie, T. Kikudome, K. Teramura, and S. Yamanaka, *J. Solid State Chem.* **182** (2009) 129.